

GT2011-458, \$

TEMPORAL AND CONVECTIVE INERTIA EFFECTS IN PLAIN JOURNAL BEARINGS WITH ECCENTRICITY, VELOCITY AND ACCELERATION

Saeid Dousti

ROMAC, University of Virginia
Charlottesville, Virginia, USA

Jianming Cao

ROMAC, University of Virginia
Charlottesville, Virginia, USA

Amir Younan

ROMAC, University of Virginia
Charlottesville, Virginia, USA

Paul Allaire

ROMAC, University of Virginia
Charlottesville, Virginia, USA

Tim Dimond

ROMAC, University of Virginia
Charlottesville, Virginia, USA

ABSTRACT

Fluid film bearings are commonly analyzed with the conventional Reynolds equation, without any temporal inertia effects, developed for oil or other high viscosity lubricants. In applications with rapidly time varying external loads, e.g. ships on wavy oceans, temporal inertia effect should be taken into account. As rotating speeds increase in industrial machines and the reduced Reynolds number increases above the turbulent threshold, a form of linearized turbulence model is often used to increase the effective viscosity to take the turbulence into account. Other than the turbulence effect, with high reduced Reynolds number, convective inertia effect gains importance. Water or other low viscosity fluid film bearings used in subsea machines and compressors are potential applications with a highly reduced Reynolds number.”

This paper extends the theory originally developed by Tichy [1] for impulsive loads to high reduced Reynolds number lubrication in different bearing configurations. Both fluid shear and pressure gradient terms are included in the velocity profiles across the lubricant film. The incompressible continuity equation and Navier Stokes equations, including the temporal inertia term, are simplified using an averaged velocity approach to obtain an extended form of Reynolds equation which applies to both laminar and turbulent flow. All terms in the Navier Stokes equation, including both the convective and temporal inertia terms are included in the analysis. The inclusion of the temporal inertia term creates a fluid acceleration term in the extended Reynolds equation. A primary advantage of this formulation is that fluid film bearings lubricated with low viscosity lubricants which are subject to high force slew rates can be analyzed with this extended Reynolds equation.

A short bearing form of the extended Reynolds equation is developed with appropriate boundary conditions. A full

kinematic analysis of the short journal bearing is developed including time derivatives up to and including shaft accelerations. Linearized stiffness, damping and mass coefficients are developed for a plain short journal bearing. A time transient solution is developed for the pressure and bearing loads in plain journal bearings supporting a symmetric rigid rotor when the rotor is subjected to rapidly applied large forces. The change in the rotor displacements when subjected to unbalance forces is explored. Several comparisons between conventional Reynolds equation solutions and the extended Reynolds number form with temporal inertia effects will be presented and discussed.

INTRODUCTION

In the conventional Reynolds equation, both temporal and convective inertia effects are neglected. This approach is easily justified in the analysis for low reduced Reynolds number and low reduced frequency number cases [2]. However, there is a significant list of applications where both temporal and convective inertia effects are important and can affect the analysis of fluid film bearings. These include high surface speed applications, low viscosity lubricants, shock loads in bearings, squeeze film dampers under impulsive loads and others.

The analysis of lubricant films to include inertia effects in lubricant films has occurred over a long period of time. Some initial efforts to define laminar, intermediate and turbulent regions of lubricant flow were reported in Pinkus and Sternlicht [3]. This approach was extended by Banerjee, Shan and Katyal [4] to form a more generalized form of Reynolds equation including inertia terms. Chen and Chen [5] investigated the effects of fluid film inertia on finite journal bearings showing that only small effects are seen for bearings

with moderate Reynolds number. Tieu [6] modeled convective inertia effects in a finite length stepped thrust bearing and found significant effects near the step.

Modeling of effects due to turbulence and convective inertia were introduced by Ng [7], Ng and Pan [8], and Elrod and Ng [9] using an eddy-diffusivity formulation including nonlinear shear and pressure gradient terms which are included in an extended form of Reynold's equation. This approach was correlated well with existing steady state experimental results and is often used in bearing modeling software. However, it only includes convective inertia effects and does not include a treatment of temporal inertia terms.

Constantinescu [10] and Constantinescu and Galatuse [11, 12] developed an alternative theory including convective inertia effects and turbulence effects using an averaged velocity over the lubricant film approach. They obtained an extended form of Reynolds equation including the effects of the convective inertia. A method of averaged inertia was also reported by Szeri, Raimondi, and Giron [13] and applied to squeeze film dampers. San Andres and Vance [14] extended this work. Reinhardt and Lund [15] developed a perturbation approach to the solution of Reynolds equation including first order terms in the reduced Reynolds number. However, this method does not converge for reduced Reynolds number greater than 1.

Tichy and Bou-Said [1] extended the formulation of Reynolds equation to include impulsive loads for the first time. They used the method of averaged velocity to obtain an extended Reynolds equation including the effects of impulsive loads for the first time. The additional terms include both additional squeeze velocity and squeeze acceleration terms. Tichy and Bou-Said presented an example analyses for pure squeeze film loads, short bearing pressure profiles, and some rigid rotor transient response plots without and with the additional temporal and convective inertia terms. Kakoty and Majumadar [16] discussed the effects of fluid inertia on oil bearing stability noting that inertia effects are significant on the rigid rotor stability values. Hashimoto et al [22] investigated the combined effect of the turbulence and fluid inertia. However, they didn't express the dynamic system matrices including the two effects. Fritz [21] also studied instability in rotor system but his equations are applied for large clearance application as in mechanical seals more than in journal bearings.

This work presents a reanalysis of the continuity and Navier Stokes equations using a similar method to Tichy and Bou-Said [1] but including the effect of linearized turbulence terms. In doing so, we find several changes which appear to be typographical errors in the Tichy and Bou-Said [1] earlier equations in the extended Reynolds equation. The extended Reynolds equation is then written in non-dimensional form in terms of reduced Reynolds number, dimensionless time and a few other parameters. Several applications of the new theory are presented. First we consider a short bearing under steady load, velocity and accelerations for several values of reduced Reynolds number. Also linearized stiffness, damping and mass coefficients are presented with low/high reduced Reynolds

number cases and with laminar/turbulent formulas for the effective viscosity in the bearing. The rigid rotor stability threshold is examined for the effects of reduced Reynolds number and turbulence. Second, we examine the effects of reduced Reynolds number and linearized turbulence on the nonlinear transient response of two identical bearings in a simple rigid rotor as it moves away from the steady state equilibrium position in the bearing due to fluid forces and unbalance forces.

PROBLEM FORMULATION

The incompressible Navier Stokes equations in fluid film journal bearings, Fig. (1), are the continuity equation and the three momentum equations.

$$\frac{\partial u}{\partial x} + \frac{\partial v}{\partial y} + \frac{\partial w}{\partial z} = 0 \quad (1)$$

$$\rho \left(\frac{\partial u}{\partial t} + u \frac{\partial u}{\partial x} + v \frac{\partial u}{\partial y} + w \frac{\partial u}{\partial z} \right) = -\frac{\partial p}{\partial x} + \mu \frac{\partial \tau_{xy}}{\partial y} \quad (2)$$

$$0 = -\frac{\partial p}{\partial y} \quad (3)$$

$$\rho \left(\frac{\partial w}{\partial t} + u \frac{\partial w}{\partial x} + v \frac{\partial w}{\partial y} + w \frac{\partial w}{\partial z} \right) = -\frac{\partial p}{\partial z} + \mu \frac{\partial \tau_{zy}}{\partial z} \quad (4)$$

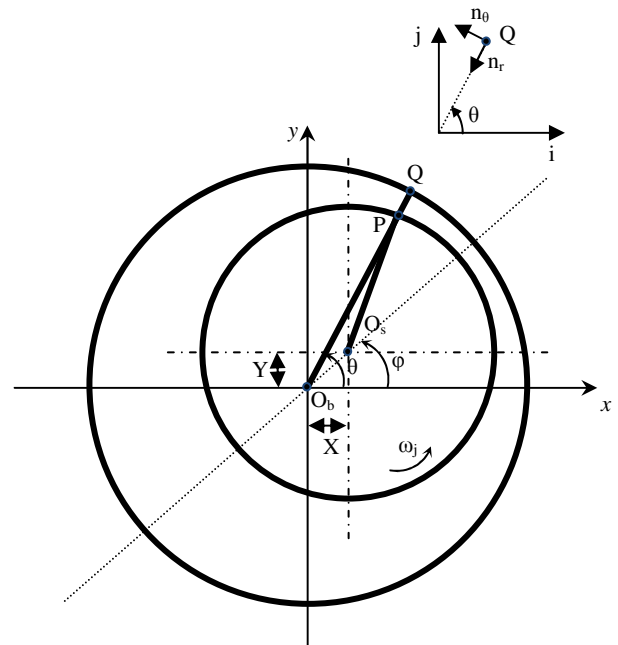


Fig 1. Plain Journal Bearing

Through a non-dimensional analysis, Szeri [13] and Kokoty [16] showed that inertia terms become important when the reduced Reynolds number (Re^*) is in the order of or greater than unity. We adopt the method of integration through

thickness suggested by Constantinescu [12]. One obtains the integrated Navier Stokes equations as

$$\frac{\partial q_x}{\partial x} + \frac{\partial q_z}{\partial z} - U \frac{\partial h}{\partial x} + V = 0 \quad (5)$$

$$\rho \left(\frac{\partial q_x}{\partial t} + \frac{\partial I_{xx}}{\partial x} + \frac{\partial I_{xz}}{\partial z} \right) = -h \frac{\partial p}{\partial x} + \tau_{xy@h} - \tau_{xy@0} + \rho U^2 \frac{\partial h}{\partial x} \quad (6)$$

$$\rho \left(\frac{\partial q_z}{\partial t} + \frac{\partial I_{xz}}{\partial x} + \frac{\partial I_{zz}}{\partial z} \right) = -h \frac{\partial p}{\partial z} + \tau_{zy@h} - \tau_{zy@0} \quad (7)$$

where q_x , q_z and I_{xx} , I_{xz} , I_{zz} represent flow rates and convective variables, respectively and are defined as

$$q_x = \int_0^h u \, dy = U_p h + \frac{1}{2} h U \quad (8)$$

$$q_z = \int_0^h w \, dy = W_p h$$

$$I_{xx} = \int_0^h u^2 \, dy$$

$$I_{xz} = \int_0^h u w \, dy \quad (9)$$

$$I_{zz} = \int_0^h w^2 \, dy$$

U_p and W_p are average velocities due to Poiseuille flow in circumferential and axial direction, respectively. U and V are journal surface velocities in circumferential and radial direction. A commonly accepted approach is to consider a parabolic velocity profile through thickness in both circumferential and axial directions [1, 12, and 16]. In this method, we assume that the effect of inertia terms on velocity profile is approximately negligible. We follow Constantinescu's method [12] based on mixing length theory to model turbulence. In his method, in the turbulent regime we still assume a parabolic velocity profile. The coefficients of convective variables are different in the laminar and turbulent regimes; we have

$$I_{xx} = \alpha U_p^2 h + \beta U^2 h + \gamma U_p U h \quad (10)$$

$$I_{xz} = U_p W_p h + \frac{1}{2} U W_p$$

$$I_{zz} = \alpha W_p^2 h$$

$$\alpha = \frac{6}{5}, \quad \beta = \frac{1}{3}, \quad \gamma = 1 \quad (11)$$

$$\alpha = 1, \quad \beta = \left(0.25 + \frac{0.885}{\text{Re}^{0.367}} \right), \quad \gamma = 1 \quad (12)$$

where Eqs. (11 and 12) specify coefficients in laminar and turbulent regime, respectively. In addition, the laminar and turbulent regime formulas for the shear are given by [12]

$$\tau_{xy@h} - \tau_{xy@0} = -\frac{k_x \mu}{h} U_p + \delta \rho \left(U_p + \frac{U}{2} \right)^2 \frac{\partial h}{\partial x} \quad (13)$$

$$\tau_{zy@h} - \tau_{zy@0} = -\frac{k_z \mu}{h} W_p$$

$$k_x = 12, \quad k_z = 12, \quad \delta = \frac{2}{15} \quad (14)$$

$$k_x = 12 + 0.0136 \text{Re}^{0.9}, \quad k_z = 12 + 0.0043 \text{Re}^{0.96} \quad (15)$$

where Eqs. (14 and 15) account for the laminar and turbulent regimes, respectively. In bearing applications, flows with $\text{Re} > 1000$ are considered as in the turbulent regime.

KINEMATIC ANALYSIS OF JOURNAL BEARING

We investigate a full kinematic analysis of short journal bearings. This includes the specification of film thickness, velocity and acceleration expressions in terms of bearing parameters and variables.

Assuming that shaft is perfectly aligned with bearing, the film thickness is defined as

$$h = c - X \cos(\theta) - Y \sin(\theta) \quad (16)$$

In fixed coordinates, the velocity vector of the journal surface is expressed as

$$\mathbf{V}_s = U \hat{n}_\theta + V \hat{n}_r = \{ R\omega - \dot{X} \sin(\theta) + \dot{Y} \cos(\theta) \} \hat{n}_\theta + \{ -\dot{X} \cos(\theta) - \dot{Y} \sin(\theta) + \omega (X \sin(\theta) - Y \cos(\theta)) \} \hat{n}_r \quad (17)$$

The over dot denotes the time derivative. This equation implies that the motion on the surface is caused by both translation and rotation of journal. Terms containing the velocities of the shaft center are translational and the ones with ω represent the rotation contribution. For instance, translational and rotational circumferential velocities are

$$U = U_r + U_t, \quad U_r = R\omega, \quad U_t = -\dot{X} \sin(\theta) + \dot{Y} \cos(\theta) \quad (18)$$

Taking the time derivative of Eq. (17), the acceleration of the shaft surface point is

$$\mathbf{a}_s = \dot{U} \hat{n}_\theta + \dot{V} \hat{n}_r = \{ -\ddot{X} \cos(\theta) - \ddot{Y} \sin(\theta) + R\omega^2 \} \hat{n}_r + \{ -\ddot{X} \sin(\theta) + \ddot{Y} \cos(\theta) - \omega^2 (X \sin(\theta) - Y \cos(\theta)) \} \hat{n}_\theta \quad (19)$$

Through Eqs. (16-18), the last two terms of integrated continuity equation Eq. (5) are simplified as follows

$$V - U \frac{\partial h}{\partial x} = \frac{\partial h}{\partial t} - U_r \frac{\partial h}{\partial x} \quad (20)$$

SHORT BEARING

Inclusion of convective inertia results in three coupled nonlinear partial differential equations Eqs. (5-7) that are difficult to solve. Finite length numerical methods solution are time consuming and computationally expensive [12,17]. Hence, we will implement our equations on short bearings, which provide sufficient tools to understand the impact of high Reynolds number phenomena on dynamical behavior of journal bearing, i.e. inertia and turbulence as well as velocity and acceleration effects. In short journal bearings, the L/D ratio is smaller than 0.5 which makes the pressure gradient in the circumferential direction negligible

$$\frac{\partial p}{\partial x} \ll \frac{\partial p}{\partial z} \quad (21)$$

Consequently, the assumption of Couette flow in the circumferential direction is reasonable and will alleviate the solution of Eq. (6), that is

$$U_p = 0 \quad q_x = \frac{1}{2} h U \quad (22)$$

Substitution of Eqs. (18, 19 and 22) in the continuity equation Eq. (5) and considering the fact that $\partial U_r / \partial x = 0$ yields

$$\frac{1}{2} \frac{\partial}{\partial x} (U_r h) + h \frac{\partial W_p}{\partial z} + \frac{\partial h}{\partial t} - \frac{\partial h}{\partial x} U_r = 0$$

$$W_p = z \Gamma(x, t) + C_1 \quad (23)$$

$$\Gamma(x, t) = -\frac{1}{h} \left(\frac{\partial h}{\partial t} + \frac{1}{2} U_r \frac{\partial h}{\partial x} + \frac{1}{2} h \frac{\partial U_r}{\partial x} - \frac{1}{2} U_r \frac{\partial h}{\partial x} \right)$$

where C_1 is constant of integration. In the above equation, terms containing U_r are in the order of C/R which can be eliminated [2]. We have

$$\Gamma(x, t) = -\frac{1}{h} \left(\frac{\partial h}{\partial t} + \frac{1}{2} U_r \frac{\partial h}{\partial x} \right) \quad (24)$$

By replacing Eqs. (8, 10, 13, 23 and 24) into Eq. (7) and differentiating once with respect to z , the modified Reynolds equation is obtained with Mathematica as

$$h^3 \frac{\partial^2 p}{\partial z^2} = k_z \mu \left(\frac{\partial h}{\partial t} + \frac{1}{2} U_r \frac{\partial h}{\partial x} \right) - \rho \left(-U_r h^2 \frac{\partial^2 h}{\partial t \partial x} - \frac{1}{4} U_r^2 h^2 \frac{\partial^2 h}{\partial x^2} \right. \\ \left. + 2\alpha U_r h \frac{\partial h}{\partial x} \frac{\partial h}{\partial t} + \frac{1}{2} \alpha U_r^2 h \left(\frac{\partial h}{\partial x} \right)^2 - h^2 \frac{\partial^2 h}{\partial t^2} + 2\alpha h \left(\frac{\partial h}{\partial t} \right)^2 \right) \quad (25)$$

Let us use dimensionless variables

$$t^* = t \omega, \quad \theta = \frac{x}{R}, \quad z^* = \frac{z}{L} \quad (26)$$

and the extended Reynolds equation is expressed as

$$h^{*3} \frac{\partial^2 p^*}{\partial z^{*2}} = k_z \left(\frac{\partial h^*}{\partial t^*} + \frac{1}{2} \frac{\partial h^*}{\partial \theta} \right) - \text{Re}^* \left(-h^{*2} \frac{\partial^2 h^*}{\partial t^* \partial \theta} - \frac{1}{4} h^{*2} \frac{\partial^2 h^*}{\partial \theta^2} \right. \\ \left. + 2\alpha h^* \frac{\partial h^*}{\partial \theta} \frac{\partial h^*}{\partial t^*} + \frac{1}{2} \alpha h^{*2} \left(\frac{\partial h^*}{\partial \theta} \right)^2 - h^{*2} \frac{\partial^2 h^*}{\partial t^{*2}} + 2\alpha h^* \left(\frac{\partial h^*}{\partial t^*} \right)^2 \right) \quad (27)$$

We note that for the laminar terms, the coefficient of the fourth right hand side (RHS) term should be 1/4 instead of 1/6 while the sixth RHS term should be -3/5 instead of -23/30 as given in Tichy and Bou-Said [1]. Since the RHS is just function of x and t , Eq. (27), along with the boundary axial boundary conditions

$$p^* \Big|_{z^* = \pm \frac{1}{2}} = 0 \quad (28)$$

can be integrated to find pressure. To take into account cavitation and film rupture when the right hand side of Eq. (27) drops below zero, pressure is considered equal to zero. The dimensionless bearing forces are calculated as

$$F_x^* = - \int_{-1/2}^{1/2} \int_{-\beta}^{\beta} p^* \cos \theta \, d\theta dz^* \quad (29)$$

$$F_y^* = - \int_{-1/2}^{1/2} \int_{-\beta}^{\beta} p^* \sin \theta \, d\theta dz^*$$

where α and β denote the circumferential angles that cavitation takes place. Obtained forces are nonlinear functions of position, velocity and also acceleration

$$F_{x,y}^* = f(X^*, Y^*, \dot{X}^*, \dot{Y}^*, \ddot{X}^*, \ddot{Y}^*) \quad (30)$$

DYNAMICAL CHARACTERISTICS AND STABILITY ANALYSIS

Beyond a specific rotational speed, bearings under constant load become unstable. To study the effect of inertia and turbulence in high Reynolds numbers on stability, we adopt the method of Allaire and Flack [18, 19] and by Kakoty [16] to formulate the nonlinear equations of motion of a rigid rotor supported by bearing as

$$\bar{m} W^* \ddot{X}^* = F_x^* \quad (31)$$

$$\bar{m} W^* \ddot{Y}^* = F_y^* - W^*$$

where W^* is the downward external load on the shaft and \bar{m} is the mass parameter which is a function of rotational speed. Under a certain external load, a stable bearing is expected to converge to a same specific equilibrium position

$$\begin{aligned} \varepsilon_0 &= (X_0^2 + Y_0^2)^{1/2} = f(W^*) \\ \phi_0 &= \tan^{-1}\left(\frac{Y_0}{X_0}\right) = f(W^*) \end{aligned} \quad (32)$$

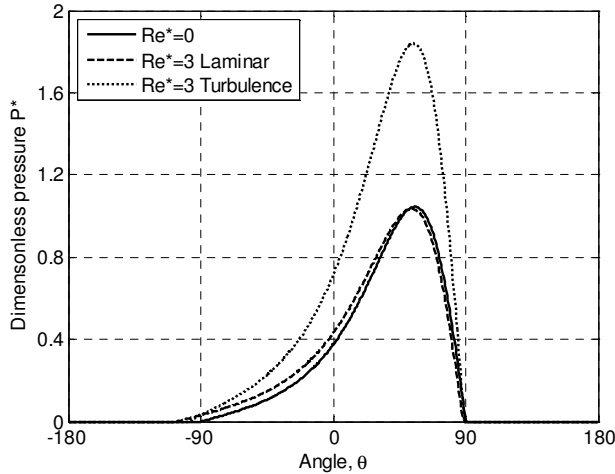
Thus, we investigate the value of \bar{m} where the bearing becomes unstable. To this aim, through a numerical perturbation method, we obtain the linearized equations of motion at equilibrium position as

$$(M_s^* + M^*)\ddot{Q}^* + C^*\dot{Q}^* + K^*Q^* = 0 \quad (33)$$

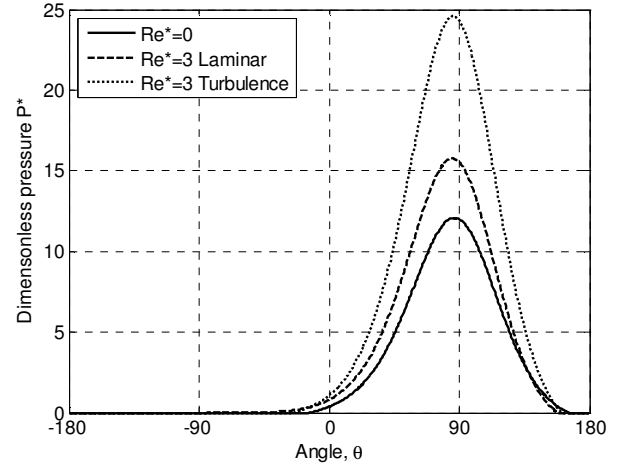
where $Q^* = [X^*, Y^*]^T$ and M^* , C^* and K^* denote dimensionless mass, damping and stiffness matrices due to hydrodynamic forces and M_s^* is shaft mass matrix

$$M_s^* = \begin{bmatrix} \bar{m}W^* & 0 \\ 0 & \bar{m}W^* \end{bmatrix} \quad (34)$$

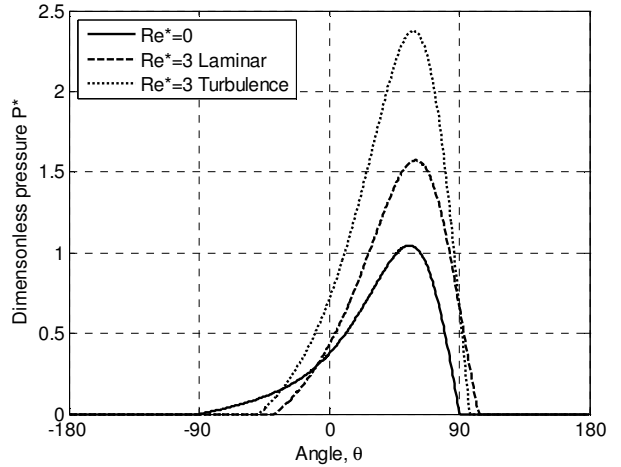
In general hydrodynamic dynamic characteristics of plain journal bearing are full matrices, i.e. having all elements non zero.



a) $\varepsilon=0.5, \partial\varepsilon/\partial t^*=\partial\phi/\partial t^*=\partial^2\varepsilon/\partial t^{*2}=\partial^2\phi/\partial t^{*2}=0$



(b) $\varepsilon=0.5, \partial\varepsilon/\partial t^*=1, \partial\phi/\partial t^*=\partial^2\varepsilon/\partial t^{*2}=\partial^2\phi/\partial t^{*2}=0$



(c) $\varepsilon=0.5, \partial\varepsilon/\partial t^*=\partial\phi/\partial t^*=\partial^2\phi/\partial t^{*2}=0, \partial^2\varepsilon/\partial t^{*2}=1$

Fig. 2 Dimensionless pressure profile $P^*(\theta, z=0)$ at different Reynolds numbers under laminar and turbulent flow and with steady state, velocity and acceleration

In Fig. 2 (a)–(c), some dimensionless pressure profiles are compared under different conditions with different reduced Reynold's number and laminar/turbulent flow. Figure 2a shows steady state pressure profiles with eccentricity 0.5 while Fig. 2b shows the case where the eccentricity is still 0.5 but a dimensionless velocity of 1 is imposed. Figure 2c shows the pressure profiles when a dimensionless acceleration of 1 is imposed.

The dimensionless forces of one journal bearing can also be rewritten as to calculate the dynamic characteristic matrices (M^* , C^* and K^*). The mass term is tied directly to the temporal inertia term in the Navier-Stokes equation as included by Tichy and Bou-Said [1991]. The Jacobian matrices of journal forces (F_x^* , F_y^*) with respect to journal displacements (X^* , Y^*), velocities (\dot{X}^* , \dot{Y}^*) and accelerations (\ddot{X}^* , \ddot{Y}^*) are

$$F^*(Q^*, \dot{Q}^*, \ddot{Q}^*) = M^* \ddot{Q}^* + C^* \dot{Q}^* + K^* Q^*$$

$$K^* = \frac{\partial F^*}{\partial Q^*} = \begin{bmatrix} \frac{\partial F_x^*}{\partial X^*} & \frac{\partial F_x^*}{\partial Y^*} \\ \frac{\partial F_y^*}{\partial X^*} & \frac{\partial F_y^*}{\partial Y^*} \end{bmatrix} = \begin{bmatrix} K_{xx}^* & K_{xy}^* \\ K_{yx}^* & K_{yy}^* \end{bmatrix}$$

$$C^* = \frac{\partial F^*}{\partial \dot{Q}^*} = \begin{bmatrix} \frac{\partial F_x^*}{\partial \dot{X}^*} & \frac{\partial F_x^*}{\partial \dot{Y}^*} \\ \frac{\partial F_y^*}{\partial \dot{X}^*} & \frac{\partial F_y^*}{\partial \dot{Y}^*} \end{bmatrix} = \begin{bmatrix} C_{xx}^* & C_{xy}^* \\ C_{yx}^* & C_{yy}^* \end{bmatrix}$$

$$M^* = \frac{\partial F^*}{\partial \ddot{Q}^*} = \begin{bmatrix} \frac{\partial F_x^*}{\partial \ddot{X}^*} & \frac{\partial F_x^*}{\partial \ddot{Y}^*} \\ \frac{\partial F_y^*}{\partial \ddot{X}^*} & \frac{\partial F_y^*}{\partial \ddot{Y}^*} \end{bmatrix} = \begin{bmatrix} M_{xx}^* & M_{xy}^* \\ M_{yx}^* & M_{yy}^* \end{bmatrix}$$

(35)

In Fig. 3-5, the variation of the dynamic characteristic matrices versus eccentricity of equilibrium position is depicted.

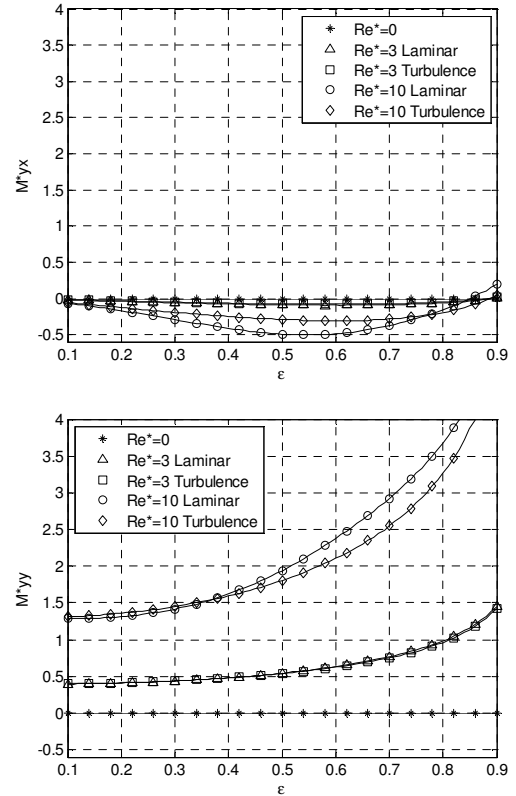
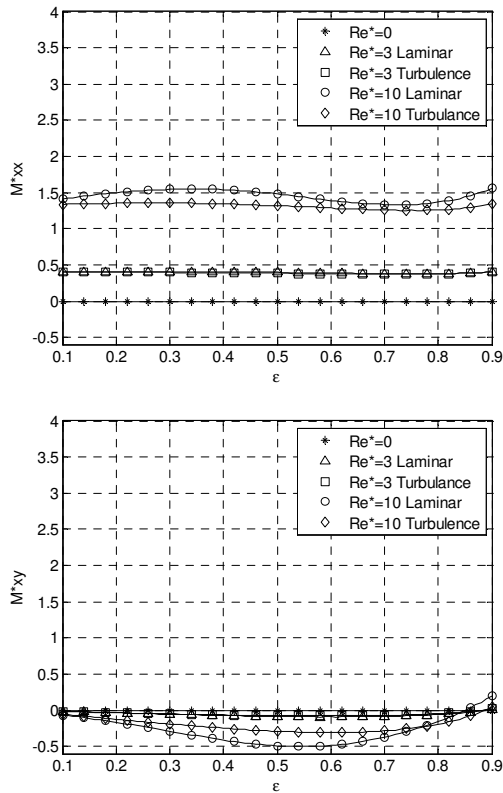
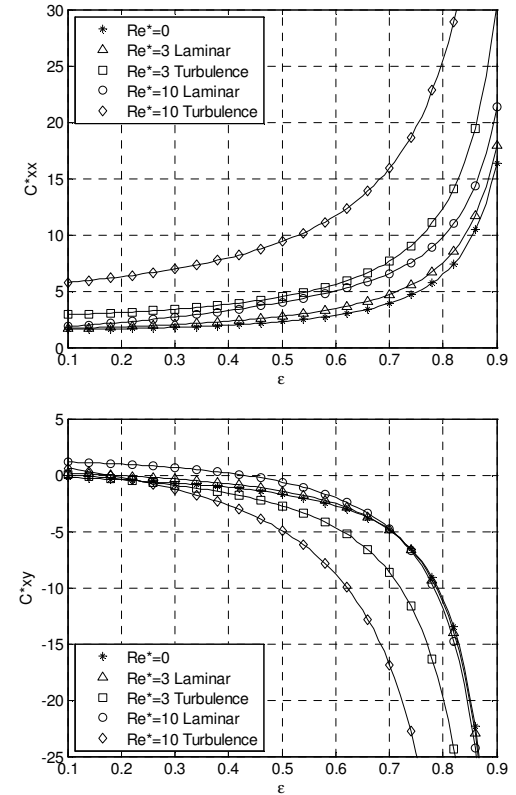


Fig. 3 Mass elements vs. equilibrium eccentricity, M_{xx}^* , M_{xy}^* , M_{yx}^* and M_{yy}^* top through bottom, respectively.



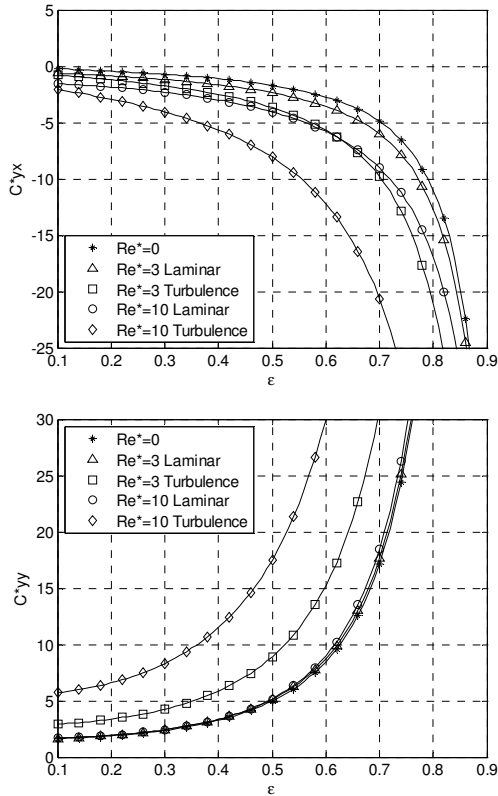


Fig. 4 Damping elements vs. equilibrium eccentricity, C_{xx}^* , C_{xy}^* , C_{yx}^* and C_{yy}^* top through bottom, respectively

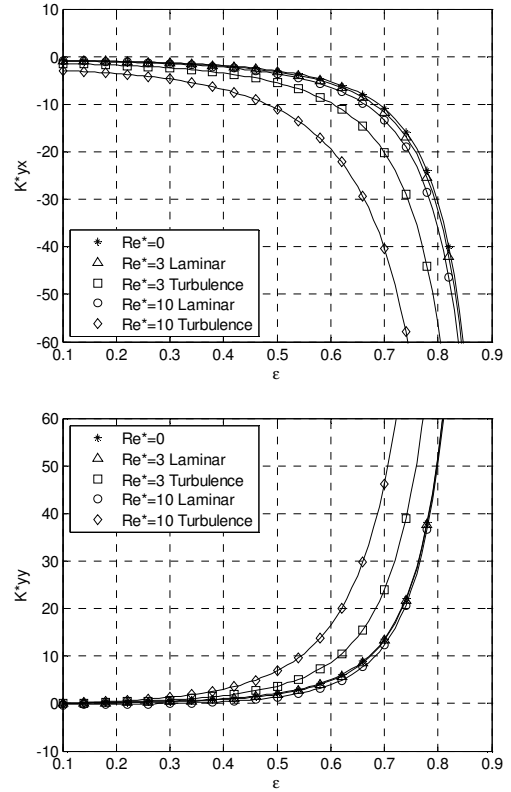
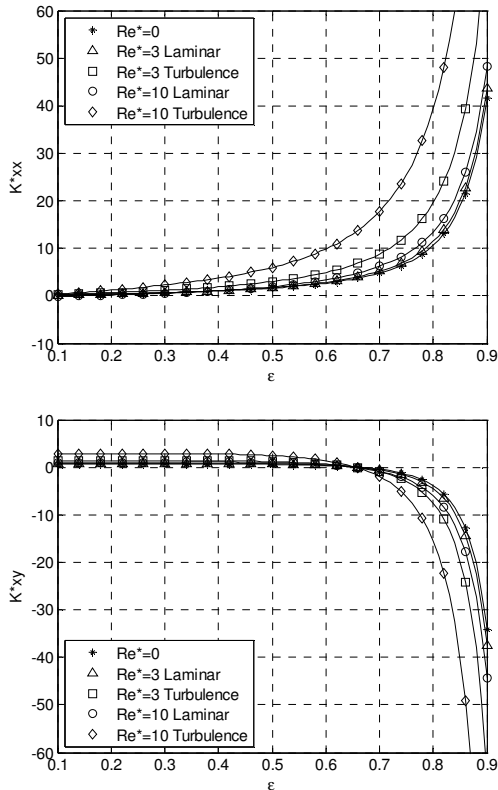


Fig. 5 Stiffness elements vs. equilibrium eccentricity, K_{xx}^* , K_{xy}^* , K_{yx}^* and K_{yy}^* top through bottom, respectively



The mass coefficients are all zero for zero reduced Reynolds number, as expected. Generally the diagonal mass terms are all positive and much larger than the off diagonal mass terms. The values increase with increasing reduced Reynolds number and turbulence. The diagonal damping terms are all positive with values increasing rapidly with eccentricity. Again the values increase with increasing reduced Reynolds number and turbulence. The stiffness terms increase with eccentricity but are not as strongly affected by increased inertia and turbulence at higher reduced Reynolds number.

The effect of fluid inertia on stability is shown in Fig.6 for a dimensionless rigid rotor stability plot as developed in Allaire and Flack [18, 19] and Majumdar and Brewe [20]. The journal center goes to a specific equilibrium position under a particular eccentricity ratio. The critical mass at a given eccentricity ratio is found when the journal center does not stay in its equilibrium position and its orbit changes from stable to unstable.

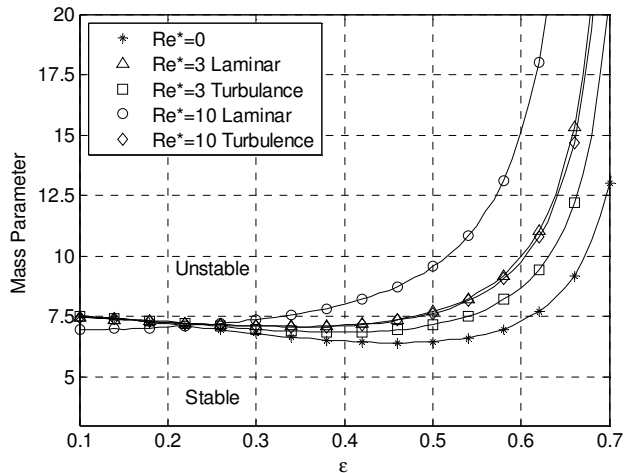


Fig. 6 Stability graph, mass parameter versus eccentricity ratio

It is seen that the effects of reduced Reynolds number of value 10 show much higher stability threshold than the case of zero. It is also interesting to note that the effect of turbulence at that same value is to reduce the stability threshold compared to the laminar case.

NONLINEAR TRANSIENT ANALYSIS OF A RIGID ROTOR

A rigid rotor, supported with two short fixed pad journal bearings at the two ends. The two have the same journal bearing geometry and the lubricant properties, which are used in the nonlinear transient analysis, are shown in Table 1. To obtain a higher reduced Reynolds number value, water is chosen as the lubricant. The parameters of the rigid rotor for transient analysis are given in Table 2.

Table 1 Short bearing geometry and properties of the lubricant

Fix Pad Short Bearing		
Property	Value	Units
Diameter	100×10^{-3}	m
Radial Clearance	0.12×10^{-3}	m
Length	50×10^{-3}	m
Water Properties		
Density	1000	kg/m^3
Viscosity	8.94×10^{-4}	Pa.s

Table 2 Transient analysis parameters for the rigid rotor

Property	Value	Units
Rigid rotor	40	kg
Unbalance Eccentricity	6×10^{-3}	kg m
Operating speed	1800	rpm
Initial Time	0	s
Final Time	.6	s
Time Step	1×10^{-4}	s

The equations of motion at X and Y direction:

$$m\ddot{X} - F_x(X, Y, \dot{X}, \dot{Y}, \ddot{X}, \ddot{Y}) - F_{xt} = 0 \quad (36)$$

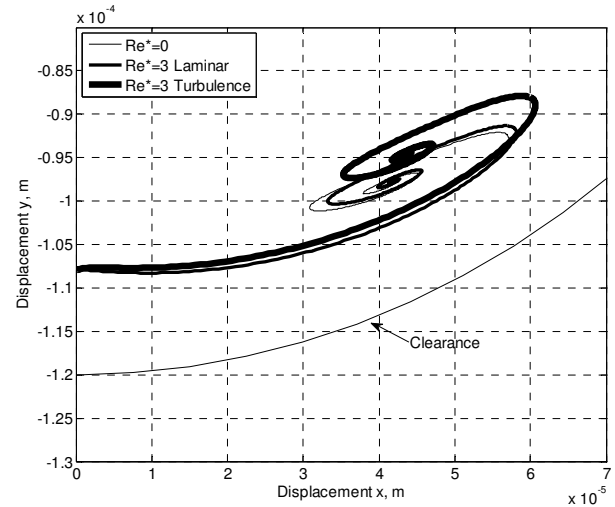
$$m\ddot{Y} - F_y(X, Y, \dot{X}, \dot{Y}, \ddot{X}, \ddot{Y}) - F_{yt} + W = 0 \quad (37)$$

The orbits of the rigid rotor at bearing with/without unbalance force at 1800 rpm are shown in Fig. 7 with values of inertia effects and flow type. The initial position of the rotor is taken at 90% of the clearance in the negative vertical direction, the start up of the machine. The final equilibrium positions and final orbits of the center of rigid rotor are different for different values of reduced Reynolds number and turbulence.

In both analyses, with and without unbalance depicted in Fig. 7, the inertia effect is observed. The forced response orbit with unbalance is elliptical. This is due to a low running speed (small unbalance forces) for this example.

Conclusions

This paper has developed a verification and extension of Tichy and Bou-Said's [1991] analysis of lubricant films including temporal inertia terms from the Navier-Stokes equation. The linearized turbulent inertia terms representing the convective inertia effects are included. The effects of these inertia terms on a short plain journal have been demonstrated in the paper. There are no published experimental results for plain journal bearings to compare these results to.



(a)

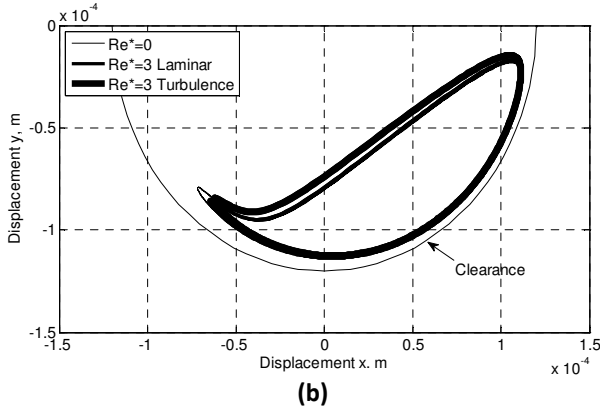


Fig. 7 Orbits of the rigid rotor at bearing at 1800rpm (a) without unbalance force and (b) with unbalance force: $Re^*=0$ (without inertia), $Re^*=3.4$ Laminar flow and $Re^*=3.4$ Turbulence flow

SOME DIMENSIONLESS GROUPS

$$F_{x,y}^* = \frac{c^2}{R L^3 \mu \omega} F_{x,y}$$

$$W^* = \frac{c^2}{R L^3 \mu \omega} W$$

$$U_r^* = \frac{U_r}{R\omega} = 1,$$

$$p^* = \frac{c^2}{L^2 \mu \omega} p$$

$$M^* = \begin{bmatrix} M_{xx}^* & M_{xy}^* \\ M_{yx}^* & M_{yy}^* \end{bmatrix}$$

$$\bar{m} = \frac{m c \omega^2}{W} : \text{mass parameter}$$

REFERENCES

- [1] Tichy, J. and Bou-Said, B., 1991, "Hydrodynamic lubrication and bearing behavior with impulsive loads", STLE Tribol. Trans., 34, pp. 505–512.
- [2] Szeri, A.Z., (1998), "Fluid Film Lubrication Theory and Design", Cambridge University Press, Cambridge.
- [3] Pinkus, O., and Sternlicht, B., 1961, "Theory of Hydrodynamic Lubrication", McGraw-Hill, New York.
- [4] Banerjee, M.B., Shandil, R. G., Katyal, S. P., Dube, G. S., Pal, T. S., Banerjee, K., 1986, "A Nonlinear Theory of Hydrodynamic Lubrication", J. Math. Anal. Appl., 117(1), pp. 48-56
- [5] Chen, Chen-Hain, and Chen, Chato-Kuang, 1989, "The Influence of Fluid Inertia on The Operating Characteristics of Finite Journal Bearings", Wear, 131, pp. 229–240
- [6] Tieu, A. K., 1986, "Turbulence and Inertia Effects in Finite Width Stepped Thrust Bearings," in Proceedings of 13th Leeds-Lyon Symposium on Tribology, Fluid Film Lubrication – Osborne Reynolds Centenary, Eds. Dowson, Taylor, Godet, and Berthe, pp. 411-416.
- [7] Ng, C.W., 1964, "Fluid Dynamic Foundation of Turbulent Flow," ASLE Trans., 7, pp. 311-321.
- [8] Ng, C.W., Pan, C.H.T., 1965, "A Linearized Turbulent Lubrication Theory," ASME J. Basic Eng., 8, pp. 675
- [9] Elrod, HG, Ng, CW, 1967, "A Theory for Turbulent Fluid Films and Its Application to Bearings," ASME J. Lubric. Tech., pp. 346-362.
- [10] Constantinescu, V. N., 1970, "On the Influence of Inertial Forces in Turbulent and Laminar Self-Acting Films", ASME J. Lubric. Tech., pp. 473-481
- [11] Constantinescu, V. N., and Galetuse, S., 1974, "On the Possibilities of Improving the Accuracy of the Evaluation of Inertia Forces in Laminar and Turbulent Films," ASME J. Lubric. Tech., 96, pp. 69–79.
- [12] Constantinescu, V. N., and Galetuse, S., 1982, "Operating Characteristics of Journal Bearings in Turbulent Inertial Flow," ASME J. Lubric. Tech., 104(1), pp. 173–179.

NOMENCLATURE

c	radial Clearance	(m)
$C_{xx}^*, \dots, C_{yy}^*$	dimensionless damping coefficients	
D	diameter of Journal	(m)
e	static displacement of eccentricity	
$\varepsilon = e/R$	eccentricity ratio	(m)
F_{x0}, F_{y0}	unbalance forces	(N)
F_x, F_y	bearing forces	(N)
F_x^*, F_y^*	dimensionless bearing forces	
h	film thickness	(m)
$h^* = h/c$	dimensionless film thickness	
$K_{xx}^*, \dots, K_{yy}^*$	dimensionless stiffness coefficients	
L	length of bearing	(m)
m	mass of shaft	(kg)
$M_{xx}^*, \dots, M_{yy}^*$	dimensionless mass coefficients	
R	shaft radius	(m)
$Re = \rho R \omega c / \mu$	Reynolds number	
$Re^* = Re c / R$	modified Reynolds number,	
t	time	(s)
U	journal surface velocity in x	(m/s)
V	journal surface radial velocity	(m/s)
U_p	average fluid velocity in x	(m/s)
W_p	average fluid velocity in z	(m/s)
q_x	flow rate in x direction	(m ² /s)
q_z	flow rate in z direction	(m ² /s)
I_{xx}, I_{yy}, I_{zz}	convective inertia variables	(m ³ s ⁻²)
x, y, z	Cartesian coordinates	(m)
X, Y	shaft center displacements	(m)
X^*, Y^*	dimensionless shaft displacements	
ω	rotation speed	(rad/s)
U_t	translational circum. velocity	(m/s)
U_r	rotational circum. Velocity	(m/s)
\mathbf{V}_s	shaft surface velocity vector	(m/s)
\mathbf{a}_s	shaft surface acceleration vector	(m/s ²)
θ	position angle in bearing coordinate	
τ_{xy}, τ_{zy}	shear Stress	(Pa)
ρ	density	(kg/m ³)

- [13] Szeri, A. Z., Raimondi, A. A. and Giron-Duarte, A. , 1983, "Linear force coefficients for squeeze-film dampers", ASME J. Lubric. Tech., 105, pp. 326-334.
- [14] San Andrés, L. and Vance, J., 1987, "Effect of Fluid Inertia on Finite Length Sealed Squeeze Film Dampers," ASLE Trans., 30, No. 3, pp. 384-393
- [15] Reinhardt, E. and Lund, J.W. , 1975, "The Influence of Fluid Inertia on the Dynamic Properties of Journal Bearings", ASME J. Lubric. Tech., 97, p. 159-167.
- [16] Kakoty, S. K. and Majumdar, B. C., 2000, "Effect of Fluid Inertia on Stability of Oil Journal Bearings", ASME J. Tribol., 122, pp. 741-745.
- [17] Lauder, B. E., and Leschziner, M. A., 1977, "An Efficient Numerical Scheme for the Prediction of Turbulent Flow in thrust Bearing", Proceedings of the 1975 Leeds-Lyon Symposium Superlaminar Flow in Bearing, I. Mech. Eng. Publications, London, pp 137-143.
- [18]Allaire, P. E., and Flack, R. D., 1980, "Journal Bearing Design for High Speed Turbomachinery, Bearing Design - Historical Aspects, Present Technology, and Future Problems", ASME, pp. 111-160.
- [19]Flack, R. D., and Allaire, P. E., 1980, "Instability Thresholds for Flexible Rotors in Hydrodynamic Bearings" in Rotor Dynamic Instability Problems in High Performance Machines, Texas A&M University, May 12-14, NASA Conference Publication 2133, pp. 403-427
- [20] Majumdar, B. C., and Brewe, D. E., 1987, "Stability of a Rigid Rotor Supported on Oil-Film Journal Bearings Under Dynamic Load", NASA Technical Memorandum 102309, AVS-COM, Technical Report 87-C-26, pp. 1-10.
- [21] Fritz, R., 1970, "The Effects of an Annular Fluid on the Vibrations of a Long Rotor: Part I Theory," ASME J. Basic Eng., 92, pp. 923-929.
- [22] Hashimoto, H., Wada, S., Sumitomo, M., 1988, "The Effects of Fluid Inertia Forces on the Dynamic Behavior of Short Journal Bearings in Superlaminar Flow Regime," ASME J. Tribol., 110(3), pp. 539-547.